Journal of Organometallic Chemistry 695 (2010) 1753–1760

Contents lists available at ScienceDirect

Journal of Organometallic Chemistry

journal homepage: www.elsevier.com/locate/jorganchem

$[(\eta^6\text{-}C_6H_6)Ru^{II}(L)(Cl/N_3/CN/CH_3CN)]^{+/2+}$ complexes of non-planar pyrazolylmethylpyridine ligands: Formation of helices due to C–H···X (X = Cl, N) interaction

Haritosh Mishra, Rabindranath Mukherjee*

Department of Chemistry, Indian Institute of Technology Kanpur, Kanpur 208 016, India

ARTICLE INFO

Article history:
Received 2 December 2009
Received in revised form
18 March 2010
Accepted 23 March 2010

Keywords:
Benzene-coordinated Ru(II)
Pyrazolylmethylpyridines
^{1}H NMR spectra
Crystal structure
Non-covalent interaction
Helical structure

ABSTRACT

Structural analysis of a previously reported half-sandwich complex having three-legged "piano-stool" geometry $[(\eta^6\text{-}C_6H_6)Ru^{II}(L^1)Cl][PF_6]$ (**1**) (L^1 = 2-(pyrazol-1-ylmethyl)pyridine) is described. Treatment of **1** with (i) $Ag(CF_3SO_3)$ in CH_3CN and (ii) NaN_3 in CH_3OH, and (iii) the reaction between $[(\eta^6\text{-}C_6H_6)Ru(L^2)Cl][PF_6]$ (**2**) (previously reported) and NaCN in C_2H_5OH led to the isolation of $[(\eta^6\text{-}C_6H_6)Ru(L^1)(CH_3CN)][PF_6]_2$ (**3**), $[(\eta^6\text{-}C_6H_6)Ru(L^1)(N_3)][PF_6]$ (**4**), and $[(\eta^6\text{-}C_6H_6)Ru(L^2)(CN)][PF_6]$ (**5**), respectively (L^2 = 2-(3,5-dimethyl-pyrazol-1-ylmethyl)pyridine). The complex $[(\eta^6\text{-}C_6H_6)Ru(L^4)Cl][PF_6]$ (**6**) with a new ligand (L^4 = 2-[3-(4-fluorophenyl)pyrazol-1-ylmethyl]pyridine) has also been synthesized. The structures of **3**–**6** have been elucidated (^{1}H NMR spectra; CD_3CN). The molecular structures of **1**, **4**, and **6**·$C_6H_5CH_3$ have been determined. Notably, the crystal-packing in these structures is governed by C–H···X (X = Cl, N) interactions, generating helical architectures.

1. Introduction

Continued interest in half-sandwich arene–ruthenium compounds [1] having "piano-stool" geometry, arises due to their (i) catalytic potential in a wide range of organic reactions [2,3] and (ii) very promising anticancer activity of $\{(\eta^6\text{-arene})Ru^{II}(L)Cl\}^+$ (L = neutral bidentate N-donor ligand) complexes both *in vitro* and *in vivo* [4,5], strengthened by non-covalent interactions [5a,5c].

In recent years considerable attention is being paid toward weak interactions such as C–H···X (X = O, F, Cl, π) and N–H···Cl, and π–π stacking between aromatic rings in directing crystal-packing topology in organometallic molecules [6–9]. Such studies on half-sandwich complexes having "piano-stool" geometry $[(\eta^6\text{-}C_6H_6)\text{-}Ru^{II}(L)Cl]^+$ (L = bidentate neutral N-donor ligand) [7], $[(\eta^6\text{-}C_6H_6)\text{-}Ru^{II}(HPz/Me_2HPz)_2Cl]^+$ (HPz/Me_2HPz = pyrazole/3,5-dimethylpyrazole) [8], and $[(\eta^6\text{-}C_6H_6)Ru^{II}(CPI)(PPh_3)Cl]^+$ (CPI = 1-(4-cyanophenyl)imidazole) [9] have revealed creation of interesting supramolecular architectures. It is worth mentioning here that among the assembly of all the supramolecular networks, helices belong to a unique class due to its ubiquitous presence in biology [10]. Although in recent years many helical networks have been reported, examples of helices fully assembled by C–H···Cl interaction are relatively scarce [11].

This work is part of our continuing efforts in the synthesis of new half-sandwich complexes of the types $[(\eta^6\text{-}C_6H_6)Ru^{II}(L)Cl]^+$ (Fig. 1) and $[(\eta^6\text{-}C_6H_6)Ru^{II}(L'/L'')]^{+/2+}$ (L = neutral bidentate planar/non-planar heterocyclic N-donor ligands [7a,12a]; L′ = mono-negative phenolate-based tridentate (2-pyridyl)alkylamine/alkyl-amine ligands [7b]; L″ = neutral tridentate (2-pyridyl)alkylamine ligands [12a]) to investigate their structure and properties (nucleophilic addition onto the Ru^{II}-coordinated benzene ring [12b,12c], electrochemical generation and stabilization of phenoxyl radical-coordinated $\{(\eta^6\text{-}C_6H_6)Ru^{II}\}^{2+}$ species [7b]), and the potential of $[(\eta^6\text{-}C_6H_6)Ru^{II}(L)Cl]^+$ complexes to involve in non-covalent interactions generating various supramolecular architectures with varying dimensionality [7a,7b]. Herein we describe (a) reactivity properties of previously reported complexes $[(\eta^6\text{-}C_6H_6)Ru^{II}(L^1)Cl][PF_6]$ (**1**) and $[(\eta^6\text{-}C_6H_6)Ru^{II}(L^2)Cl][PF_6]$ (**2**) (L^1 = 2-(pyrazol-1-ylmethyl)pyridine; L^2 = 2-(3,5-dimethyl-pyrazol-1-ylmethyl)pyridine), (b) nucleophilic halide displacement/substitution reactions of **1**and **2** with $Ag(CF_3SO_3)$, NaN_3 or NaCN to synthesize $[(\eta^6\text{-}C_6H_6)\text{-}Ru^{II}(L^1)(CH_3CN)][PF_6]_2$ (**3**), $[(\eta^6\text{-}C_6H_6)Ru^{II}(L^1)(N_3)][PF_6]$ (**4**), and $[(\eta^6\text{-}C_6H_6)Ru^{II}(L^2)(CN)][PF_6]$ (**5**), and structural characterization of **4**, and (c) synthesis and properties of a new complex $[(\eta^6\text{-}C_6H_6)Ru^{II}(L^4)\text{-}$

* Corresponding author. Tel.: +91 512 2597437; fax: +91 512 2597436.
E-mail address: rnm@iitk.ac.in (R. Mukherjee).

0022-328X/$ – see front matter © 2010 Published by Elsevier B.V.
doi:10.1016/j.jorganchem.2010.03.022

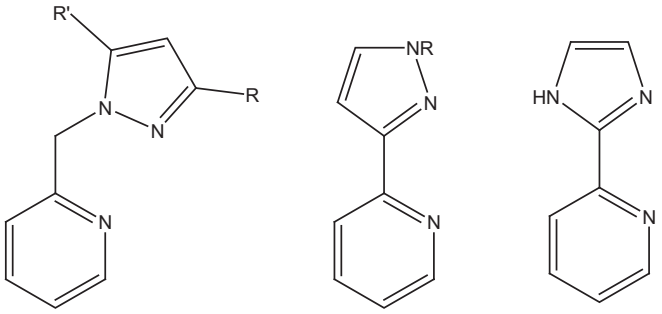

R = R' = H ($\mathbf{L^1}$)
R = R' = Me ($\mathbf{L^2}$)
R = -C_6H_4-*p*-Cl, R' = H ($\mathbf{L^3}$)
R = -C_6H_4-*p*-F, R' = H ($\mathbf{L^4}$)

R = H ($\mathbf{HL^5}$)
= -CH_2-C_6H_5 ($\mathbf{L^6}$)

$\mathbf{HL^7}$

Fig. 1. The ligands of pertinence to this work.

Cl][PF_6] (**6**) (L^4 = 2-[3-(4-fluorophenyl)pyrazol-1-ylmethyl]pyridine), and X-ray structure of **6**·$C_6H_5CH_3$. The crystal structure of [(η^6-C_6H_6)-Ru^{II}(L^3)Cl][PF_6] (L^3 = 2-[3-(4-chlorophenyl)pyrazol-1-ylmethyl]-pyridine) has already been reported [7a]. Notably, the complexes considered here generate helical structures via C–H···Cl–Ru, C–H···F–C, and C–H···N_3–Ru interactions.

2. Experimental

2.1. Materials

Reagent or analytical grade chemicals were obtained from commercial sources and used, without further purification. The ligands 2-(pyrazol-1-ylmethyl)pyridine (L^1) [13], 2-(3,5-dimethyl-pyrazol-1-ylmethyl)pyridine (L^2) [13], and the dimer [{(η^6-C_6H_6)Ru^{II}(μ-Cl)Cl}$_2$] [14] were prepared following reported procedures.

2.2. Preparation of ligand

2.2.1. 2-[3-(4-Fluorophenyl)pyrazol-1-ylmethyl]pyridine (L^4)

The starting material 3-(4-fluorophenyl)-1-pyrazole necessary for the synthesis of L^4 was prepared following a procedure similar to that used for the synthesis of L^3 [7a]. A solution of 1-(4-fluoro-phenyl)ethanone (2.0 g, 0.013 mol) in *N*,*N*-dimethylformamide dimethylacetal [4.7 g (5 mL), 0.039 mol] was refluxed for 10 h. After cooling to 298 K, the excess of solvent was removed under a reduced pressure. The resulting sticky solid was dried in vacuo and used in the next step without further purification. Yield: 1.64 g (~70%). A mixture of the resulting compound 1-(4-fluorophenyl)-but-2-en-1-one (1.64 g, 0.009 mol) and hydrazine hydrate [4.5 g (4 mL), 0.09 mol] in C_2H_5OH (3 mL) was stirred at 333 K for 30 min. After cooling to 298 K, the reaction mixture was poured into 20 g of ice which afforded a white precipitate. It was filtered, washed with cold water several times, and dried in air. Recrystallization from a mixture (1:2; v/v) of chloroform/*n*-hexane afforded a white crystalline solid. Yield: 1.04 g (65%). ^{1}H NMR ($CDCl_3$; 80 MHz; 298 K): 6.32 (d, 1H, pyrazole H^4), 7.30–7.58 (m, 4H, benzene), 7.65 (d, 1H, pyrazole H^5).

A mixture of 2-(chloromethyl)pyridine hydrochloride (0.92 g, 5.62 mmol), 3-(4-fluorophenyl)-1-pyrazole (1.0 g, 5.62 mmol), benzene (60 mL), 40% aqueous NaOH (8 mL), and 40% aqueous tetra-*n*-butylammonium hydroxide (8 drops) was refluxed with stirring for 8 h and then stirred at 298 K for 12 h. The organic layer was then separated, washed twice with brine water (100 mL), dried over anhydrous $MgSO_4$, and filtered. Solvent removal afforded a thick yellowish white solid. Yield: 1.06 g (~70%). The ligand was further purified by recrystallization from chloroform/*n*-hexane. ^{1}H NMR ($CDCl_3$; 80 MHz; 298 K): δ 5.42 (s, 2H, CH_2), 6.54 (d, 1H, pyrazole H^4), 7.00–7.68 (m, 7H, pyridine $H^{3,4,5}$ and phenyl $H^{2,3,5,6}$), 7.80 (d, 1H, pyrazole H^5), 8.62 (d, 1H, pyridine H^6).

2.3. Syntheses of complexes

The complexes [(η^6-C_6H_6)Ru^{II}(L^1)Cl][PF_6] (**1**) and [(η^6-C_6H_6)Ru^{II}(L^2)Cl][PF_6] (**2**) were prepared as before [12a]. X-ray quality single-crystals of **1** were obtained by diffusion of diethyl ether into a solution of the complex in a mixture (1:5; v/v) of CH_3OH and CH_3CN.

2.3.1. [(η^6-C_6H_6)Ru(L^1)(CH_3CN)][PF_6]$_2$ (**3**)

To a solution of **1** (0.102 g, 0.2 mmol) in CH_3CN (10 mL) was added $Ag(CF_3SO_3)$ (0.051 g, 0.2 mmol). The mixture was then refluxed for 4 h. A white precipitate of AgCl appeared which was discarded. To the lemon yellow filtrate solid NH_4PF_6 (0.032 g, 0.2 mmol) was added. The volume of the solution was reduced to ~3 mL by evaporation. Addition of diethyl ether precipitated the product, which was filtered, washed with a mixture (1:5; v/v) of CH_3CN and diethyl ether, and dried under vacuum. The product was recrystallized from a mixture (1:5; v/v) of CH_3CN and diethyl ether. Yield: 0.096 g (70%). Anal. Calc. for $C_{17}H_{18}N_4P_2F_{12}Ru$ (**3**): C, 30.50; H, 2.71; N, 8.37. Found: C, 30.59; H, 2.70; N, 8.34%. IR (KBr, cm^{-1}): 2327 ν(CH_3CN), 839 ν(PF_6^-). ^{1}H NMR (CD_3CN; 400 MHz; 298 K): δ 9.04 (d, J_{HH} = 5.6 Hz, 1H, H^6 of py), 8.14 (t, 1H, J_{HH} = 7.9 Hz, 1H, H^4 of py), 8.04 (d, 2H, J_{HH} = 6.6 Hz, 2H, $H^{3'}$ and $H^{5'}$ of pz), 7.78 (d, J_{HH} = 6.6 Hz, 1H, H^3 of py), 7.60 (t, J_{HH} = 7.3 Hz, 1H, H^5 of py), 6.61 (t, J_{HH} = 6.6 Hz, 1H, $H^{4'}$ of pz), 6.21 (s, 6H, C_6H_6), 5.74 (d, J_{gem} = 15.9 Hz, 1H, NCH_2–), 5.28 (d, J_{gem} = 16.1 Hz, 1H, NCH_2–), 2.33 (s, 3H, CH_3CN). Molar conductance, Λ_M (CH_3CN, 298 K) = 118 Ω^{-1} cm^2 mol^{-1}. UV–Vis (in CH_3CN): λ/nm (ε/dm^3 mol^{-1} cm^{-1}) 264 (4600), 270 sh (3500), 300 sh (670), 370 (330).

2.3.2. [(η^6-C_6H_6)Ru(L^1)(N_3)][PF_6] (**4**)

To a solution of **1** (0.102 g, 0.2 mmol) in CH_3OH (10 mL) was added solid NaN_3 (0.013 g, 0.2 mmol) and the mixture was refluxed for 5 h. During this period the color of the solution changed from yellow to orange. On cooling, an orange crystalline solid that formed was filtered, washed with cold CH_3OH, and dried under vacuum. The product was recrystallized from hot CH_3OH solution as an orange crystalline solid. X-ray diffraction-quality crystals were obtained by diffusion of diethyl ether into a solution of the complex in CH_3CN. Yield: 0.070 g (70%). Anal. Calc. for $C_{15}H_{15}N_6PF_6Ru$ (**4**): C, 34.29; H, 2.88; N, 16.00. Found: C, 34.36; H, 2.89; N, 16.14%. IR (KBr, cm^{-1}): 2035 ν(N_3^-), 839 ν(PF_6^-). ^{1}H NMR (CD_3CN; 400 MHz; 298 K): δ 8.98 (d, J_{HH} = 5.36 Hz, 1H, H^6 of py), 8.03 (t, J_{HH} = 7.8 Hz, 1H, H^4 of py), 7.95 (d, J_{HH} = 6.8 Hz, $H^{3'}$ and $H^{5'}$ of pz), 7.67 (d, J_{HH} = 7.8 Hz, 1H, H^3 of py), 7.54 (t, J_{HH} = 6.1 Hz, 1H, H^5 of py), 6.56 (t, J_{HH} = 6.8 Hz, 1H, $H^{4'}$ of pz), 5.90 (s, 6H, C_6H_6), 5.67 (d, J_{gem} = 15.6 Hz, 1H, NCH_2–), 5.39 (d, J_{gem} = 15.6 Hz, 1H, NCH_2–). Molar conductance, Λ_M (CH_3CN, 298 K) = 118 Ω^{-1} cm^2 mol^{-1}. UV–Vis (in CH_3CN): λ/nm (ε/dm^3 mol^{-1} cm^{-1}) 240 sh (11 000), 266 (8500), 390 (850).

2.3.3. [(η^6-C_6H_6)Ru(L^2)(CN)][PF_6] (**5**)

To a solution of **2** (0.102 g, 0.2 mmol) in C_2H_5OH (10 mL) was added solid NaCN (0.0098 g, 0.2 mmol). The mixture was refluxed for 5 h and the color of the solution changed from yellow to orange. On cooling, an orange crystalline solid that formed was filtered, washed with cold CH_3OH, and dried under vacuum. The product was recrystallized by diffusion of diethyl ether into a solution of the complex in a mixture (2:1; v/v) of CH_3CN and CH_3OH. Yield: 0.080 g

(75%). Anal. Calc. for $C_{18}H_{19}N_4PF_6Ru$ (**5**): C, 40.23; H, 3.56; N, 10.43. Found: C, 40.36; H, 3.62; N, 10.54%. IR (KBr, cm^{-1}): 2057 $\nu(CN^-)$, 839 $\nu(PF_6^-)$. ^1H NMR (CD_3CN; 400 MHz; 298 K): δ = 9.10 (d, J_{HH} 5.6 Hz, 1H, H_6 of py), 7.99 (t, J_{HH} 8.0 Hz, 1H, H^4 of py), 7.69 (d, J_{HH} = 7.6 Hz, 1H, H^3 of py), 7.49 (t, J_{HH} = 6.2 Hz, 1H, H_5 of py), 6.13 (s, 1H, $H^{4\prime}$ of pz), 5.92 (s, 6H, C_6H_6), 5.47 (d, J_{gem} = 16.0 Hz, 1H, NCH_2–), 5.13 (d, J_{gem} = 15.6 Hz, 1H, NCH_2–), 2.50 (s, 3H, 5-CH_3 of pz), 2.41 (s, 3H, 3-CH_3 of pz). Molar conductance, Λ_M (MeCN, 298 K) = 224 Ω^{-1} cm^2 mol^{-1}. UV–Vis (in CH_3CN): λ/nm (ϵ/dm^3 mol^{-1} cm^{-1}) 230 sh (9150), 270 (4050), 385 (1100).

2.3.4. [(η^6-C_6H_6)$Ru^{II}(L^4)Cl$][PF_6] (**6**)

L^4 (0.084 g, 0.4 mmol) was dissolved in CH_3OH (15 mL) and to it was added solid [{(η^6-C_6H_6)Ru^{II}(μ-Cl)Cl}$_2$] (0.100 g, 0.2 mmol). The mixture was stirred for 12 h at 298 K. The resulting yellow solution was filtered and the volume of the filtrate was reduced (~7 mL) and to it solid NH_4PF_6 (0.065 g, 0.4 mmol) was added. The yellow microcrystalline solid that formed was filtered, washed with cold CH_3OH, and dried in vacuo. Recrystallization was achieved from hot CH_3OH solution. Yield: 0.130 g (57%). Anal. Calc. for $C_{21}H_{18}ClF_7N_3PRu$ (**6**): C, 41.15; H, 2.96; N, 6.86. Found: C, 40.94; H, 2.94; N, 6.81%. IR (KBr, cm^{-1}): 841 $\nu(PF_6^-)$. ^1H NMR (CD_3CN; 400 MHz; 298 K): δ 9.09 (d, J_{HH} = 6.8 Hz, 1H, H^6 of py), 8.04 (t, J_{HH} = 7.6 Hz, 1H, H^4 of py), 7.99 (d, J_{HH} = 7.2 Hz, 1H, $H^{5\prime}$ of pz), 7.77. (m, 3H, H^5 of py, $H^{3\prime\prime}$, $H^{4\prime\prime}$ of phenyl), 7.68 (d, J_{HH} = 7.8 Hz, 1H, H_3 of py) 7.56, 7.52 (t, J_{HH} = 7.2 Hz, 1H, H^5 of py), 7.26 (m, 2H, $H^{2\prime\prime}$, $H^{5\prime\prime}$ of phenyl), 6.54 (d, J_{HH} = 7.2 Hz, 1H, $H^{4\prime}$ of pz), 5.67 (s, 6H, C_6H_6), 5.67 (1H, –CH_2–, overlaps with C_6H_6 resonance), 5.42 (d, J_{gem} = 15.6 Hz, 1H, –CH_2–). Molar conductance, Λ_M (CH_3CN, 298 K) = 150 Ω^{-1} cm^2 mol^{-1}. UV–Vis (in CH_3CN): λ/nm (ϵ/dm^3 mol^{-1} cm^{-1}) 265 (8500), 295 (3500), 415 (450). X-ray quality single-crystals of composition **6**·$C_6H_5CH_3$ were obtained by layering of toluene on a solution of the complex in a mixture of CH_3CN and CH_2Cl_2.

2.4. Instrumentation

Elemental analyses were obtained using Thermo Quest EA 1110 CHNS-O, Italy. Conductivity measurements were done with an Elico type CM-82T conductivity bridge (Hyderabad, India). Spectroscopic measurements were made using the following instruments: IR (KBr, 4000–600 cm^{-1}), Bruker Vector 22; electronic, Perkin Elmer Lambda 2 and Agilent 8453 diode-array spectrophotometer. ^1H NMR spectral measurements were performed on a JEOL-JNM-LA-400 FT (400 MHz) NMR spectrometer.

2.5. Crystal structure determination

Diffraction intensities were collected either on an Enraf Nonius CAD-4-mach four-circle diffractometer at 298(2) K (**1**) or on a Bruker SMART APEX CCD diffractometer at 100(2) K (**4** and **6**·$C_6H_5CH_3$) using graphite-monochromated Mo Kα (λ = 0.71073 Å) radiation. Intensity data were corrected for Lorentz polarization effects. Empirical absorption correction (SADABS) was applied. The structures were solved by SIR-97, expanded by Fourier-difference syntheses, and refined with SHELXL-97, incorporated in WinGX 1.64 crystallographic collective package [15]. Hydrogen atoms were placed in idealized positions, and treated using riding model approximation with displacement parameters derived from those of the atoms to which they were bonded. All non-hydrogen atoms were refined with anisotropic thermal parameters by full-matrix least-squares procedures on F^2. A summary of the data collection and structure refinement information is provided in Table 1. Intermolecular contacts of the C–H···Cl and C–H···N types were examined with the DIAMOND package [16]. C–H distances were normalized along the same vectors to the neutron derived values of 1.083 Å [17].

Table 1
Data collection and structure refinement parameters for [(η^6-C_6H_6)$Ru^{II}(L^1)$Cl][PF_6] (**1**), [(η^6-C_6H_6)$Ru^{II}(L^1)(N_3)$][PF_6] (**4**), and [(η^6-C_6H_6)$Ru^{II}(L^4)$Cl][PF_6] (**6**·$C_6H_5CH_3$).

	1	**6**·$C_6H_5CH_3$	**4**
Chemical formula	$C_{15}H_{15}ClF_6N_3PRu$	$C_{28}H_{26}ClF_7N_3Pru$	$C_{15}H_{15}F_6N_6PRu$
M	518.79	705.01	525.37
Crystal color, habit	Yellow, needle	Yellow, block	Orange, block
T, K	293(2)	100(2)	100(2)
Cryst system	Tetragonal	Orthorhombic	Orthorhombic
Space group	$I4_1/a$ (#88)	$P2_12_12_1$ (#19)	$P2_12_12_1$ (#19)
a/Å	22.928(5)	12.991(5)	10.818(5)
b/Å	22.928(5)	13.105(5)	12.803(5)
c/Å	14.181(5)	16.376(5)	13.402(5)
α/°	90.0	90.0	90.0
β/°	90.0	90.0	90.0
γ/°	90.0	90.0	90.0
V/Å^3	7455(3)	2788.0(17)	1856.2(13)
Z	16	4	4
d_{calcd}/g cm^{-3}	1.849	1.680	1.880
μ/mm^{-1}	1.133	0.787	1.004
F(000)	4096	1416	1040
No. of reflns collected	6592	18075	12189
No. of indep reflns [R (int)]	3248 [0.0897]	6809 [0.0342]	4577 [0.0165]
No. of reflns used [$I > 2\sigma(I)$]	2043	6238	4567
GOF on F^2	1.014	1.104	1.185
Final R indices [$I > 2\sigma(I)$][a,b]	0.0604, 0.1513	0.0350, 0.0694	0.0267, 0.0634
Final R indices (all data)	0.1073, 0.1779	0.0426, 0.0890	0.0268, 0.0634

[a] $R_1 = \Sigma(|F_o| - |F_c|)/\Sigma|F_o|$.
[b] $wR_2 = \{\Sigma[w(|Fo|^2 - |Fc|^2)^2]/\Sigma[w(|Fo|^2)^2]\}^{1/2}$.

3. Results and discussion

3.1. The complexes and their general characterization

In our previous work, we presented the molecular structures of half-sandwich complexes of the type [(η^6-C_6H_6)Ru^{II}(L)Cl]$^+$ [7a] having piano-stool geometry using a series of neutral bidentate N-donor ligands [two heterocycles directly attached, thus allowing the rings to electronically communicate (HL^5, L^6, and HL^7) and also with a non-planar ligand L^3, in which two heterocycles are separated by a methylene spacer, thus preventing electronic communication between the two rings] (Fig. 1). The present work is concerned with non-planar bidentate N-donor ligands (L^1, L^2, and L^4), giving us an opportunity to (i) investigate the effect of these ligands on the structure and bonding aspects of half-sandwich complexes of composition {(η^6-C_6H_6)Ru^{II}(L)Cl}$^+$ (L represents bidentate neutral N-donor ligands) and (ii) to look for generalizations from the standpoint of non-covalent interactions [6–9,11,17–22].

Treatment of previously reported complex [(η^6-C_6H_6)$Ru^{II}(L^1)$Cl]-[PF_6] (**1**) [12a] with (i) $Ag(CF_3SO_3)$ in CH_3CN and (ii) NaN_3 in CH_3OH, and (iii) the reaction between previously reported complex [(η^6-C_6H_6)$Ru(L^2)$Cl][PF_6] (**2**) [12a] and NaCN in C_2H_5OH led to the isolation of complexes [(η^6-C_6H_6)$Ru(L^1)(CH_3CN)$][PF_6]$_2$ (**3**), [(η^6-C_6H_6)$Ru(L^1)(N_3)$][PF_6] (**4**), and [(η^6-C_6H_6)$Ru(L^2)(CN)$][PF_6] (**5**), respectively (Scheme 1). Reaction of the dimer [{(η^6-C_6H_6)Ru^{II}(μ-Cl)Cl}$_2$] [14] with L^4 in CH_3OH in the presence of NH_4PF_6 afforded isolation of a new complex [(η^6-C_6H_6)$Ru(L^4)$Cl][PF_6] (**6**). It has to be stressed here that the ligand L^4 present in **6** was deliberately designed to investigate the effect of a fluorine atom in **6**·$C_6H_5CH_3$ in the place of a chlorine atom present in L^3 ligand in [(η^6-C_6H_6)-$Ru^{II}(L^3)$Cl][PF_6] [7a]. We anticipated that owing to small size and high electronegativity of fluorine, the C–F bond would be a better candidate than C–Cl to participate in C–H···X (X = Cl or F) interactions. Thus complex **6**·$C_6H_5CH_3$ is an ideal candidate to explore

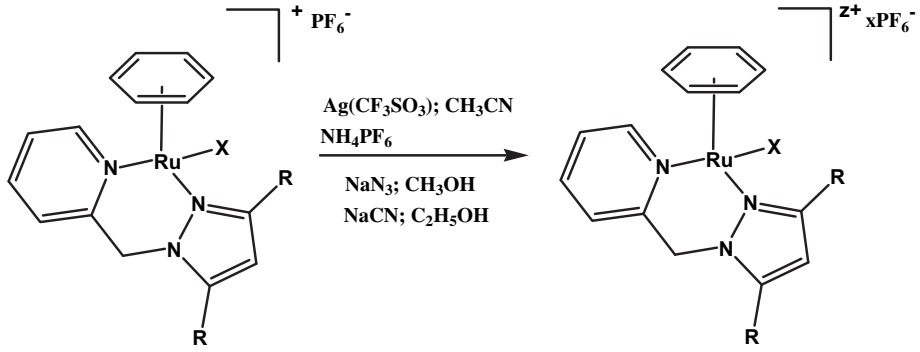

Scheme 1.

the participation of both C–H···Cl [6b,6e,6g,7a,8,9,11,17–20] and C–H···F [6e,6g,9,21] interactions.

Characterization of the new complexes was accomplished by elemental analysis, solution electrical conductivity, IR and ^{1}H NMR spectroscopy. Consistent with their formulation, IR stretching vibration of PF_6^- at ~840 cm^{-1} confirms cationic nature of the complexes **3**–**6**. IR spectra of the solvent-bound complex **3** and anion-bound complexes **4**, **5**, and **6** show common features, in addition to attesting to the vibrations expected due to the presence of coordinated CH_3CN, N_3^-, and CN^-. Conductivity studies revealed that **3**, **5**, and **6** behave as 1:1 electrolyte and **3** as 1:2 electrolyte [23].

Complexes **3**–**6** exhibit absorption spectral band at 415, 365, 390, and 388 nm, respectively.

3.2. Molecular structures of $[(\eta^6\text{-}C_6H_6)Ru(L^1)Cl][PF_6]$ (**1**), $[(\eta^6\text{-}C_6H_6)Ru(L^1)(N_3)][PF_6]$ (**4**), and $[(\eta^6\text{-}C_6H_6)Ru(L^4)Cl][PF_6]\cdot C_6H_5CH_3$ (**6**·$C_6H_5CH_3$)

In order to confirm the identity and chelate-ring conformation of the coordinated ligands, single-crystal X-ray structure determination was done for the chloride-bound complexes **1** and **6**·$C_6H_5CH_3$, and azide-bound complex **4**. X-ray crystallographic analysis confirms the structure of the complexes (Fig. 2 and Table 2). The cations exhibit the expected and usual pseudo-octahedral half-sandwich "piano-stool" disposition around the Ru(II) cation [1c,7–9,26], with the benzene ligand occupying one face of the octahedron (the Ru(II) center is π-bonded to the η^6-C_6H_6 group) and the coordination of a bidentate heterocyclic N-donor ligand [N(1) of pyridine and N(3) of pyrazole] and a chloride (**1**, **6**·$C_6H_5CH_3$) or azide (**4**) ion on the other face.

The N–Ru–N angles have values of 83.7(3)° (**1**), 88.04(14)° (**6**·$C_6H_5CH_3$), and 86.03(10)° (**4**), deviated from 90° as per demand of the bite of the ligand.

In **1** and **6**·$C_6H_5CH_3$ the pyridyl mean plane is tilted to adjacent pyrazole ring at an angle of 55.116(11)° and 46.38(6)°, respectively, attesting their non-planar nature [24,25]. In addition, the pyrazole ring and *p*-fluourophenyl group of L^4 in **6**·$C_6H_5CH_3$ make an angle of 70.07(6)°.

It is worth mentioning here that although several examples of structurally characterized mononuclear half-sandwich complexes having $\{(\eta^6\text{-}C_6H_6)Ru\}^{2+}$ unit are now known [1c,7–9,26], the number of structurally characterized complexes of the type "$[(\eta^6\text{-}C_6H_6)Ru(L)(S/X)]^{z+}$" (L = neutral bidentate heterocyclic N-donor ligands containing either both soft donors [26h] (six-membered nitrogen heterocycle pyridine due to its π-electron deficiency behaves as excellent π-acceptors and in turn they provide soft site for metal coordination) or combination of both a soft pyridine and a hard pyrazole (the π-excessive five-membered nitrogen heterocycle pyrazole is a poorer π-acceptor. In fact, it is a better π-donor and hence acts as hard donor site) [7a]; S = solvent and X = monodentate anion); z = 1 for X and z = 2 for S) is scarce. The obvious effect of these donor sites (non-planar pyrazolylmethylpyridine ligands) to the properties of the resulting complexes is the differential flow of electron density from the bidentate ligands to the $\{(\eta^6\text{-}C_6H_6)Ru^{II}Cl\}^+$ moieties. This in turn modulates (i) the electron density on the Ru^{II}-coordinated benzene ring (^{1}H NMR spectra) and (ii) the hydrogen-bonding donor properties of Ru^{II}-coordinated chloride ion and the hydrogen-bonding acceptor properties of various C–H moieties present on the ligand backbone (see below).

3.3. Comparison of metric parameters

For complexes **1** and **6**·$C_6H_5CH_3$ the observed trend in Ru–C, Ru–N(py) (py = pyridine), Ru–N(pz) (pz = pyrazole), and Ru–Cl distances (Table 3), reflecting mutual trans influence, is a consequence of interplay between steric and electronic factors associated with the coordinating ability of bidentate ligands L^1 or L^4, in a closely similar metal coordination environment.

Average Ru–C distances in **1**, **6**·$C_6H_5CH_3$, and **4** (Table 2) compare well with that reported in the literature [1c,8,26c,26g], including our previous report [7a] on similar three-legged piano-stool complexes having $\{(\eta^6\text{-}C_6H_6)Ru^{II}Cl\}^+$ moiety. The Ru–N(py) and Ru–N(pz) bond lengths in **1**, **6**·$C_6H_5CH_3$, and **4** (Table 3) also compare well with reported values [8,26a,26e], including our previous report [7a]. The Ru–Cl distances in **1** and **6**·$C_6H_5CH_3$ are comparable to that reported in the literature for closely similar complexes [1c,8,26c,26e,26g], including our previous observation [7a]. The Ru–N(azide) bond length in **5** is comparable to that reported in the literature for a closely similar three-legged piano-stool complex [1c]. The average Ru–C distance [2.191(3) Å] in **4** is longer than [2.158(10) Å] in **1**. It might be due to greater trans influence of the azide ion compared to the chloride ion [the azide ion is a stronger σ-donor than chloride ion because Ru–N (azide) bond length is much shorter (~0.3 Å) than that of Ru–Cl bond lengths (Tables 2 and 3)].

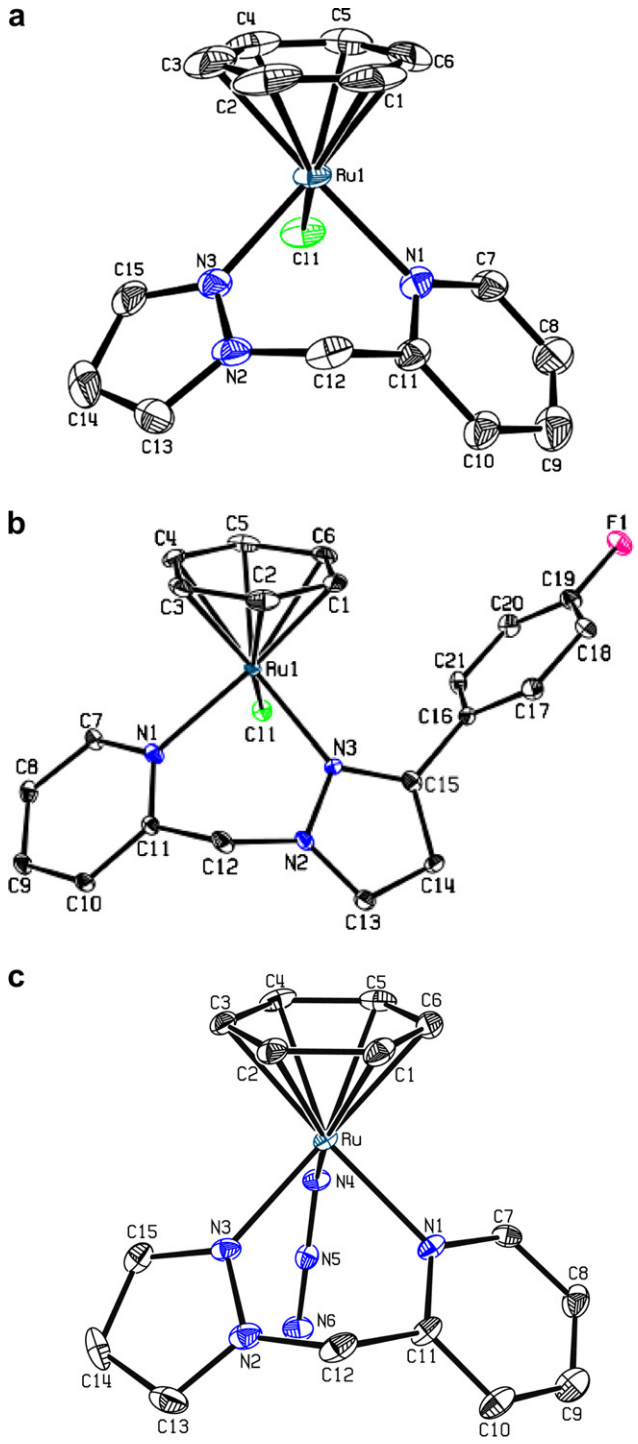

Fig. 2. Perspective views of (a) $[(\eta^6\text{-}C_6H_6)Ru^{II}(L^1)Cl]^+$ in **1**, (b) $[(\eta^6\text{-}C_6H_6)Ru^{II}(L^4)Cl]^+$ in **6**·$C_6H_5CH_3$, and (c) $[(\eta^6\text{-}C_6H_6)Ru^{II}(L^1)(N_3)]^+$in **4**. Hydrogen atoms have been omitted for clarity.

3.4. ^1H NMR spectra

The new complexes (**3**–**6**) were characterized by ^1H NMR spectroscopy. The data in CD_3CN along with their assignments are recorded in the Experimental Section, supporting their expected "piano-stool" structure [Figs. S1–S4 (Supplementary material)]. The proton resonances were assigned based on the available ^1H NMR spectral results for the free ligands [13], and those for closely similar complexes [7a,12a]. Formation of the complexes provides rigidity to the ligand structure. In essence, the ^1H NMR results clearly indicate that the solid state structures (vide supra) are retained in solution.

Table 2
Selected bond lengths (Å) and angles (°) in $[(\eta^6\text{-}C_6H_6)Ru^{II}(L^1)Cl][PF_6]$ (**1**), $[(\eta^6\text{-}C_6H_6)Ru^{II}(L^1)(N_3)][PF_6]$ (**4**), and $[(\eta^6\text{-}C_6H_6)Ru^{II}(L^4)Cl][PF_6]\cdot C_6H_5CH_3$ (**6**·$C_6H_5CH_3$).

	1	**6**·$C_6H_5CH_3$	**4**
Ru(1)–N(1)	2.111(7)	2.122(3)	2.112(3)
Ru(1)–N(3)	2.087(6)	2.091(3)	2.087(3)
Ru(1)–Cl(1)	2.386(2)	2.4025(12)	–
Ru(1)–N(4)	–	–	2.107(2)
Ru(1)–C(1)	2.155(11)	2.177(4)	2.192(3)
Ru(1)–C(2)	2.150(9)	2.189(4)	2.188(3)
Ru(1)–C(3)	2.180(12)	2.168(4)	2.194(3)
Ru(1)–C(4)	2.151(10)	2.189(4)	2.181(3)
Ru(1)–C(5)	2.151(10)	2.181(5)	2.193(3)
Ru(1)–C(6)	2.161(10)	2.190(4)	2.198(3)
C(1)–C(2)	1.390(20)	1.423(7)	1.403(5)
C(2)–C(3)	1.355(19)	1.392(6)	1.425(4)
C(3)–C(4)	1.317(17)	1.413(7)	1.398(5)
C(4)–C(5)	1.359(18)	1.381(6)	1.421(5)
C(5)–C(6)	1.340(18)	1.426(7)	1.399(5)
C(1)–C(6)	1.460(20)	1.379(8)	1.416(5)
N(1)–Ru–N(3)	83.7(3)	88.04(14)	86.03(10)
N(1)–Ru–Cl(1)	85.14(18)	81.66(9)	–
N(3)–Ru–Cl(1)	86.60(19)	85.79(9)	–
N(1)–Ru–N(4)	–	–	84.31(9)
N(3)–Ru–N(4)	–	–	85.47(10)

3.5. Non-covalent interaction

A closer inspection of the crystal-packing diagrams of **1**, **4**, and **6**·$C_6H_5CH_3$ reveals that these organometallic molecules are engaged in interesting non-covalent interactions (see below). Relevant bond distances and bond angles are summarized in Table 4, which are in good agreement with prior results [5c,6,8,9,17,18,20–22], including our own findings [7a,11,12].

3.5.1. $[(\eta^6\text{-}C_6H_6)Ru(L^1)Cl][PF_6]$ (**1**) and $[(\eta^6\text{-}C_6H_6)Ru(L^4)Cl][PF_6]\cdot C_6H_5CH_3$ (**6**·$C_6H_5CH_3$)

In **1** intermolecular C–H···Cl hydrogen-bonding interaction [5c,6,7a,8,9,11,18] linking the neighboring molecules gives rise to a 1D helical architecture [11] along the *c* axis (Fig. 3).The Ru^{II}-coordinated chloride ion is involved in hydrogen-bonding interaction with C–H(2) of the benzene ring of a neighboring molecule.

In **6**·$C_6H_5CH_3$ intermolecular C–H···Cl interactions link the neighboring molecules to give rise to a 1D helical architecture along the *a* axis (Fig. 4). Here the Ru^{II}-coordinated Cl^- ion is involved in interaction with the methylene C–H of L^4 of a neighboring molecule. The 1D helical chains thus formed in turn are involved in C–H···F contacts with molecules in the adjacent layer, involving C–H of pyridine ring and the organic fluorine atom F(1) present in

Table 3
Summary of relevant bond distances (Å) in $[(\eta^6\text{-}C_6H_6)Ru^{II}(L^1)Cl][PF_6]$ (**1**), $[(\eta^6\text{-}C_6H_6)\text{-}Ru^{II}(L^1)(N_3)][PF_6]$ (**4**), and $[(\eta^6\text{-}C_6H_6)Ru^{II}(L^4)Cl][PF_6]\cdot C_6H_5CH_3$ (**6**·$C_6H_5CH_3$).

	1	**6**·$C_6H_5CH_3$	**4**
Av Ru–C	2.158(10)	2.182(2)	2.191(4)
Ru–C_6H_6 centroid	1.667	1.672	1.677
Av C–C	1.370(16)	1.402(7)	1.410(6)
Ru–N(py)	2.111(7)	2.122(3)	2.112(3)
Ru–N(pz)	2.087(6)	2.091(3)	2.087(3)
Ru–N(azide)	–	–	2.107(2)
Ru–Cl	2.386(2)	2.4025(12)	–

Table 4
Hydrogen-bonding (C–H···Cl/N) parameters for $[(\eta^6\text{-}C_6H_6)Ru^{II}(L^1)Cl]^+$ in **1**, $[(\eta^6\text{-}C_6H_6)Ru^{II}(L^1)(N_3)]^+$ in **4** and $[(\eta^6\text{-}C_6H_6)Ru^{II}(L^4)Cl]^+$ in **6**·$C_6H_5CH_3$.

D–H···*A*	H···*A*, Å	*D*···*A*, Å	*D*–H···*A*
$[(\eta^6\text{-}C_6H_6)Ru^{II}(L^1)Cl]^+$ unit in **1**			
C2–H2···Cl1	2.739[a]	3.621(10)	158.7°[b]
$[(\eta^6\text{-}C_6H_6)Ru^{II}(L^4)Cl]^+$ unit in **6**·$C_6H_5CH_3$			
C12–H12B···Cl	3.001	3.5547(10)	114.8°[c]
C10–H10···F	2.5598	3.2328(9)	123.9°[c]
$[(\eta^6\text{-}C_6H_6)Ru^{II}(L^1)(N_3)]^+$ unit in **4**			
C3–H3···N6	2.434[b]	3.290(6)	134.9°[d]
C15–H15···N6	2.533[c]	3.552 (10)	156.4°[e]

[a] $0.25 + y, 1.25 - x, 0.25 + z$.
[b] $1.25 - y, -0.25 + x, -0.25 + z$.
[c] $x, 1 + y, z$.
[d] $0.5 + x, 0.5 - y, 1 - z$.
[e] $-0.5 + x, 0.5 - y, 1 - z$.

p-fluorophenyl group of L^4. Such interactions result in the formation of a 2D hydrogen-bonded network (Fig. S5).

3.5.2. $[(\eta^6\text{-}C_6H_6)Ru(L^1)(N_3)][PF_6]$ (**4**)

The crystal-packing diagram of **4** reveals that the cation $[(\eta^6\text{-}C_6H_6)Ru(L^1)(N_3)]^+$ is engaged in non-covalent interaction. Like the helical structures observed in the case of **1** and **6**·$C_6H_5CH_3$, compound **4** also gives rise to a 1D helical architecture along the *a* axis, via intermolecular C–H···N hydrogen bonds (Fig. 5). In fact, the azide nitrogen N(6) is involved in bifurcated hydrogen-bonding interaction with H(3) of the benzene ring and with H(15) of pyrazole ring of a neighboring molecule. The hydrogen-bonding parameters observed here [2.532(23) Å and 137.1°; 2.655(3) Å and 157.6°] fall in the range observed in the literature (C–H···N: 2.522–2.721 Å; 124.6–157.3°) [22].

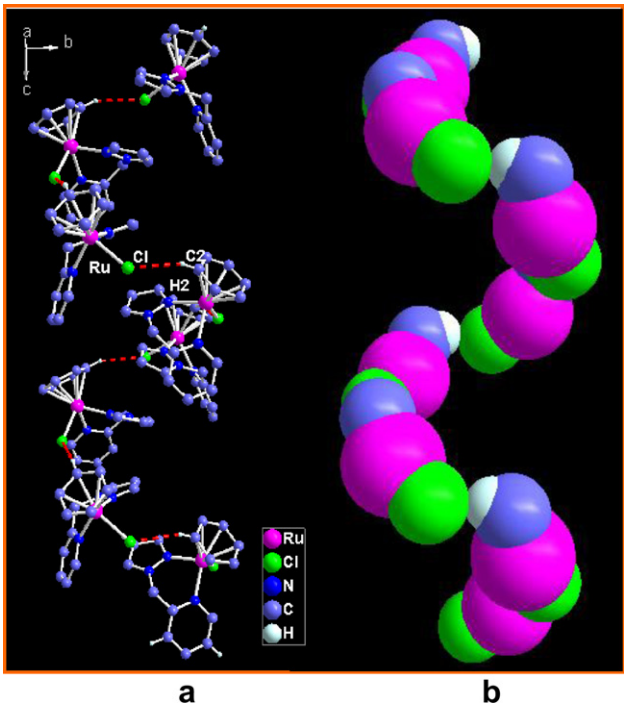

Fig. 3. (a) View of helix formation through C–H ··· Cl hydrogen-bonding in $[(\eta^6\text{-}C_6H_6)Ru(L^1)Cl]^+$ unit in **1**. All the hydrogen atoms except those involved in hydrogen bonding have been omitted for clarity. (b) Space-filling view of inner channel running parallel to the helical axis.

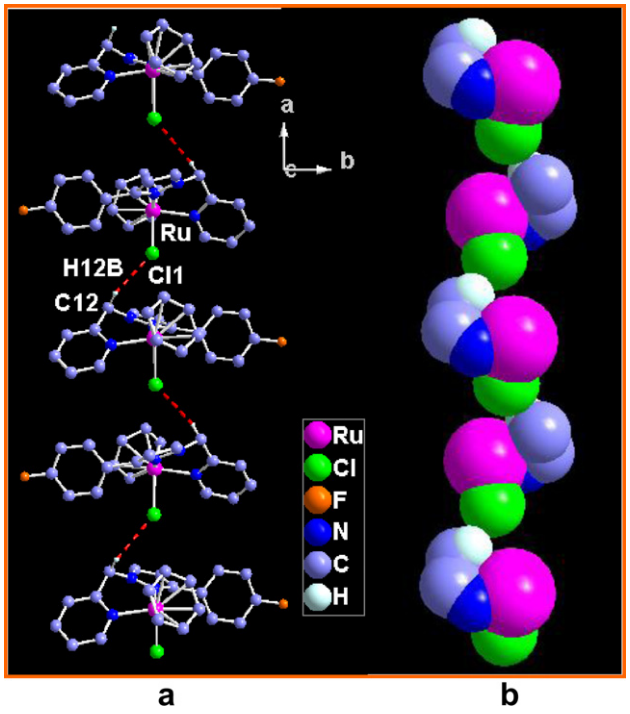

Fig. 4. (a) View of helix formation through C–H ··· Cl hydrogen-bonding in $[(\eta^6\text{-}C_6H_6)Ru(L^4)Cl]^+$ unit in (**6**·$C_6H_5CH_3$). All the hydrogen atoms except those involved in hydrogen bonding have been omitted for clarity. (b) Space-filling view of inner channel running parallel to the helical axis.

3.5.3. Rationalization of observed non-covalent interaction

Inspection of the non-covalent interaction which results in the formation of supramolecular architecture (Figs. 3–5) has led us to present the following hypotheses. (i) From literature reports [6g,7a,8,9] and the present work it has been observed that the Ru^{II}-coordinated Cl^- ion in half-sandwich complexes with "piano-stool" geometry acts as an efficient hydrogen bond acceptor to engage in C–H···Cl interaction. (ii) From the point of view of charge density (it should be mentioned here that there exists no spectroscopic or other evidence for consideration of electron density related to the C–H···Cl and C–H···N interactions; the following description of charge distribution is purely based on fundamental considerations) on the coordinated benzene ring, which is tuned by the extent of donation of electron density to the Ru^{II} ion. The rings are deactivated when comparatively weak donor sites provide "three-legged" coordination. This will cause the C–H groups of Ru^{II}-coordinated C_6H_6 to be ideally suited to take part in C–H···(Cl or N) interactions. This has been realized in this work, as before [7a]. (iii) Considering charge distribution in the pyridine ring present in L^1 and L^4, which is tuned by the withdrawal of electron density from the ring-carbon atoms towards the nitrogen atom for donation to the metal ion, the rings are deactivated. This causes the positions 4 and 6 electron-deficient, and such C–H groups would thereby be ideally suited to take part in C–H···Cl interaction. This has been observed in this work. (iv) For pyrazole groups present in L^1 and L^4, 3- and 5-positions are electron-deficient [7a,11a]. The contribution of stereochemistry should, however, not be ignored (the 3 and 5 positions on the pyrazole ring are much more sterically demanding than other positions). Therefore, the involvement of pyrazole 5-H in C–H···Cl interaction observed here justifies our hypothesis. (v) We have shown in our previous reports [11] that within the framework of C–H···Cl interactions the geometry of the complex plays a vital role in the helix formation, the tetrahedral geometry favors the helix formation through hydrogen-bonding interaction.

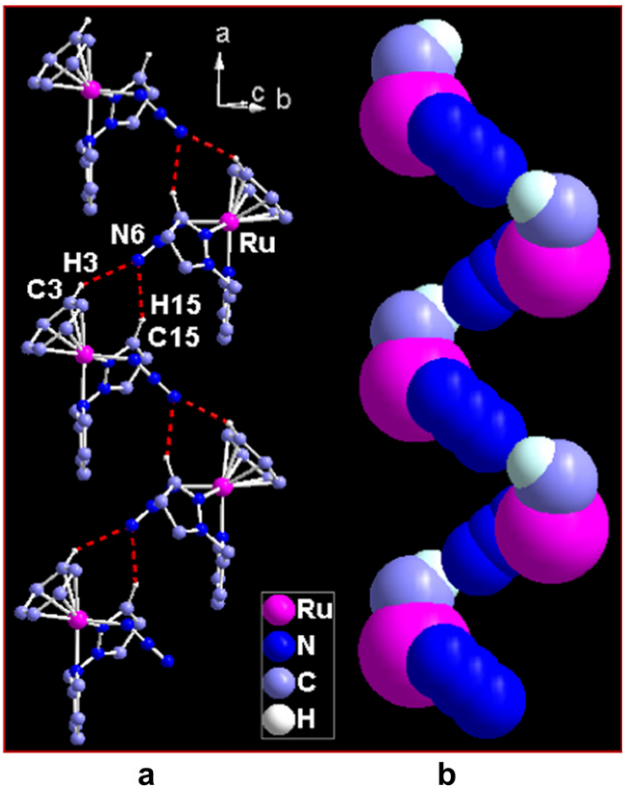

Fig. 5. (a) View of helix formation through C–H···N hydrogen-bonding in $[(\eta^6\text{-}C_6H_6)\text{-}Ru^{II}(L^1)(N_3)]^+$ unit in the crystal of **4**. All the hydrogen atoms except those involved in hydrogen bonding have been omitted for clarity. (b) Space-filling view of inner channel running parallel to the helical axis.

Considering benzene ring as a single donor group, all the Ru^{II} complexes, having three-legged "piano-stool" geometry, can be considered to assume distorted pseudo-tetrahedral geometry at the metal center. The observed results justify our hypothesis. Previously [7a] we identified a large variety of non-covalent interactions using planar bidentate ligands. Such interactions afforded network structures but helix formation was not observed [7a]. The present work demonstrates that the non-planar nature of the given ligand plays a crucial role in helix formation through non-covalent interaction. The methylene spacer which separates the two donor units (pyridine and pyrazole in L^1 and L^4) provides the required turn for the helix formation due to proper angular disposition of the interacting hydrogen atom(s).

The ligands L^3 and L^4 are almost identical. However, the crystal-packing diagrams of $\mathbf{6}\cdot C_6H_5CH_3$ and $[(\eta^6\text{-}C_6H_6)Ru^{II}(L^3)Cl][PF_6]$ [7a] are very different. In the latter case [7a] we observed only the formation of a dimeric motif, involving C–H···Cl interaction. Notably, the dimeric motif gives rise to a double helical architecture through weak C–H···Cl interactions [Fig. S6 (Supplementary material)]. Moreover, in none of the cases with planar ligands we observed helix formation through non-covalent interaction [7a]. Given the results in hand we are inclined to believe that the presence of both a five-membered and a six-membered hetrocyclic ring separated by a methylene spacer imparting non-planarity in $L^1/L^3/L^4$ (Fig. 1 and Fig. S5) has contributed to the observation of helix formation through symmetry-assisted C–H···X (Cl or N) interactions.

4. Conclusions

Despite several examples of structurally characterized mononuclear three-legged half-sandwich complexes of type $\{(\eta^6\text{-}C_6H_6)\text{-}Ru^{II}(L)Cl\}^+$ (L = neutral bidentate heterocyclic N-donor hybrid ligands), few systematic studies have been made to design this class of half-sandwich complexes with the intention of pinpointing critical roles that the ancillary ligands play in fine-tuning structure-bonding properties of these organometallic molecules. In this work a particular attention has been placed to non-planar bidentate N-donor ligands with two different heterocyclic rings. The ligands used in this work carry sites suitable for linking molecules preferentially through non-covalent interactions. Nucleophilic chloride displacement reaction and ligand substitution reaction of $[(\eta^6\text{-}C_6H_6)Ru^{II}(L^1/L^2)Cl][PF_6]$ with $Ag(O_3SCF_3)$ and NaN_3/NaCN to prepare $CH_3CN/N_3^-/CN^-$-bound complexes have also been achieved. In continuation of our previous observation we discover that Ru-coordinated benzene rings and non-planar bidentate ligands chosen here had a pronounced tendency to participate in non-covalent interactions (C–H···Cl and C–H···N) in the solid state, generating helical architectures. The present study thus provides further information pertinent to a better understanding of the non-covalent interactions in the structure directing organometallic unit $[(\eta^6\text{-}C_6H_6)Ru^{II}(L)Cl]^+$.

Acknowledgements

Financial assistance received from the Department of Science and Technology (DST), Government of India is gratefully acknowledged. HM gratefully acknowledges University Grants Commission (UGC), New Delhi for a Senior Research Fellowship. RM sincerely thanks the DST for the award of JC Bose fellowship. We thank Dr Apurba Kumar Patra for the crystal structure of complex **1**.

Appendix. Supplementary data

CCDC 736278, 290123, and 736277 contain the supplementary crystallographic data for **1**, **4**, and $\mathbf{6}\cdot C_6H_5CH_3$, respectively. These data can be obtained free of charge via http://www.ccdc.cam.ac.uk/conts/retrieving.html, or from the Cambridge Crystallographic Data Centre, 12 Union Road, Cambridge CB2 1EZ, UK; fax: (+44) 1223-336-033; or e-mail: deposit@ccdc.cam.ac.uk. Supplementary data associated with this article can be found, in the online version, at doi:10.1016/j.jorganchem.2010.03.022.

References

[1] (a) H. Le Bozec, D. Touchard, P.H. Dixneuf, Adv. Organomet. Chem. 29 (1989) 163–247;
(b) M.A. Bennett, Coord. Chem. Rev. 166 (1997) 225–254;
(c) F. Marchetti, C. Pettinari, R. Pettinari, A. Cerquetella, A. Cingolani, E.J. Chan, K. Kozawa, B.W. Skelton, A.H. White, R. Wanke, M.L. Kuznetsov, L.M.D.R. S. Martins, A.J.L. Pombeiro, Inorg. Chem. 46 (2007) 8245–8257;
(d) F. Marchetti, C. Pettinari, R. Pettinari, A. Cerquetella, C. Di Nicola, A. Macchloni, D. Zuccaccla, M. Monari, F. Piccinelli, Inorg. Chem. 47 (2008) 11593–11603.
[2] (a) R. Noyori, S. Hashiguchi, Acc. Chem. Res. 30 (1997) 97–102;
(b) T. Naota, H. Takaya, S.-I. Murahashi, Chem. Rev. 98 (1998) 2599–2660.
[3] (a) D. Carmona, M.P. Lamata, L.A. Oro, Eur. J. Inorg. Chem. (2002) 2239–2251;
(b) H. Brunner, T. Zwack, M. Zabel, W. Beck, A. Böhm, Organometallics 22 (2003) 1741–1750;
(c) J. Hannedouche, G.J. Clarkson, M. Wills, J. Am. Chem. Soc. 126 (2004) 986–987;
(d) A.J. Davenport, D.L. Davies, J. Fawcett, D.R. Russell, Dalton Trans. (2004) 1481–1492;
(e) M.C. Carrión, F.A. Jalón, B.R. Manzano, A.M. Rodríguez, F. Sepúlveda, M. Maestro, Eur. J. Inorg. Chem. (2007) 3961–3973.
[4] (a) Y.K. Yan, M. Melchart, A. Habtemariam, P.J. Sadler, Chem. Commun. (2005) 4764–4776;
(b) M. Auzias, B. Therrien, G. Süss-Fink, P. Štěpnička, W.H. Ang, P.J. Dyson, Inorg. Chem. 47 (2008) 578–583.
[5] (a) H. Chen, J.A. Parkinson, S. Parsons, R.A. Coxall, R.O. Gould, P.J. Sadler, J. Am. Chem. Soc. 124 (2002) 3064–3082;
(b) F. Wang, H. Chen, S. Parsons, I.D.H. Oswald, J.E. Davidson, P.J. Sadler, Chem. Eur. J. 9 (2003) 5810–5820;

(c) R. Fernandez, M. Melchart, A. Habtemariam, S. Parsons, P.J. Sadler, Chem. Eur. J. 10 (2004) 5173–5179;
(d) A. Habtemariam, M. Melchart, R. Fernández, S. Parsons, I.D.H. Oswald, A. Parkin, F.P.A. Fabbiani, J.E. Davidson, A. Dawson, R.E. Aird, D.I. Jodrell, P. J. Sadler, J. Med. Chem. 49 (2006) 6858–6868;
(e) T. Bugercic, A. Habtemariam, J. Stepankova, P. Heringova, J. Kasparkova, R. J. Deeth, R.D.L. Johnstone, A. Prescimone, A. Parkin, S. Parsons, V. Brabec, P. J. Sadler, Inorg. Chem. 47 (2008) 11470–11486.

[6] (a) D. Braga, F. Grepioni, G.R. Desiraju, J. Organomet. Chem. 548 (1997) 33–43;
(b) D. Braga, S.M. Draper, E. Champeil, F. Grepioni, J. Organomet. Chem. 573 (1999) 73–77;
(c) G.R. Desiraju, J. Chem. Soc. Dalton Trans. (2000) 3745–3751;
(d) L. Brammer, J.C.M. Rivas, R. Atencio, S. Fang, F.C. Pigge, J. Chem. Soc. Dalton Trans. (2000) 3855–3867;
(e) D. Braga, L. Maini, M. Polito, E. Tagliavini, F. Grepioni, Coord. Chem. Rev. 246 (2003) 53–71;
(f) L. Brammer, Chem. Soc. Rev. 33 (2004) 476–489;
(g) A. Singh, M. Chandra, A.N. Sahay, D.S. Pandey, K.K. Pandey, S.M. Mobin, M. C. Puerta, P. Valerga, J. Organomet. Chem. 689 (2004) 1821–1834;
(h) S.K. Singh, M. Chandra, D.S. Pandey, J. Organomet. Chem. 689 (2004) 2073–2079;
(i) S.K. Singh, M. Chandra, D.S. Pandey, M.C. Puerta, P. Valerga, J. Organomet. Chem. 689 (2004) 3612–3620.

[7] (a) H. Mishra, R. Mukherjee, J. Organomet. Chem. 691 (2006) 3545–3555;
(b) H. Mishra, R. Mukherjee, J. Organomet. Chem. 692 (2007) 3248–3260.

[8] J.G. Małecki, J.O. Dziegielewski, M. Jaworska, R. Kruszynski, T.J. Bartczak, Polyhedron 23 (2004) 885–894.

[9] S.K. Singh, M. Trivedi, M. Chandra, A.N. Sahay, D.S. Pandey, Inorg. Chem. 43 (2004) 8600–8608.

[10] (a) J.-M. Lehn, Supramolecular Chemistry. Concepts and Perspectives. VCH, Weinheim, 1995;
(b) M. Albrecht, Chem. Rev. 101 (2001) 3457–3497;
(c) C. Schmuck, Angew. Chem. Int. Ed. 42 (2003) 2448–2452.

[11] (a) V. Balamurugan, M.S. Hundal, R. Mukherjee, Chem. Eur. J. 10 (2004) 1683–1690;
(b) V. Balamurugan, R. Mukherjee, CrystEngComm 7 (2005) 337–341;
(c) A.K. Sharma, R. Mukherjee, Inorg. Chim. Acta 361 (2008) 2768–2776.

[12] (a) Z. Shirin, R. Mukherjee, J.F. Richardson, R.M. Buchanan, J. Chem. Soc. Dalton Trans. (1994) 465–469;
(b) Z. Shirin, A. Pramanik, P. Ghosh, R. Mukherjee, Inorg. Chem. 35 (1996) 3431–3433;
(c) H. Mishra, A.K. Patra, R. Mukherjee, Inorg. Chim. Acta 362 (2009) 483–490.

[13] D.A. House, P.J. Steel, A.A. Watson, Aust. J. Chem. 39 (1986) 1525.

[14] R.A. Zelonka, M.C. Baird, Can. J. Chem. 50 (1972) 3063–3072.

[15] L.J. Farrugia, WinGX Ver 1.64, an Integrated Systems of Windows Programs for the Solution, Refinement and Analysis of Single-crystal X-ray Diffraction Data. Department of Chemistry, University of Glasgow, 2003.

[16] DIAMOND ver 2.1c, Crystal Impact GbR, Bonn, Germany, 1999.

[17] (a) G.R. Desiraju, T. Steiner, The Weak Hydrogen Bond in Structural Chemistry and Biology. Oxford University Press, Oxford, 1999;
(b) T. Steiner, Angew. Chem. Int. Ed. 41 (2002) 48–76.

[18] (a) V. Balamurugan, W. Jacob, J. Mukherjee, R. Mukherjee, CrystEngComm 6 (2004) 396–400;
(b) V. Balamurugan, R. Mukherjee, Inorg. Chim. Acta 359 (2006) 1376–1382;
(c) V. Balamurugan, J. Mukherjee, M.S. Hundal, R. Mukherjee, Struct. Chem. 18 (2007) 133–144;
(d) V. Mishra, F. Lloret, R. Mukherjee, Eur. J. Inorg. Chem. (2007) 2161–2170;
(e) W. Jacob, R. Mukherjee, J. Chem. Sci. 120 (2008) 447–453;
(f) W. Jacob, H. Mishra, S. Pandey, F. Lloret, R. Mukherjee, New J. Chem. 33 (2009) 893–901.

[19] (a) C.B. Aakeröy, A.M. Beatty, Aust. J. Chem. 54 (2001) 409–421;
(b) L. Brammer, in: G.R. Desiraju (Ed.), Perspectives in Supramolecular Chemistry–Crystal Design: Structure and Function, vol. 7, Wiley, Chichester, 2003, pp. 1–75.

[20] (a) R. Taylor, O. Kennard, J. Am. Chem. Soc. 104 (1982) 5063–5070;
(b) G. Aullón, D. Bellamy, L. Brammer, E.A. Bruton, A.G. Orpen, Chem. Commun. (1998) 653–654;
(c) C.B. Aakeröy, T.A. Evans, K.R. Seddon, I. Pálinkó, New J. Chem. (1999) 145–152;
(d) P.K. Thallapally, A. Nangia, CrystEngComm 27 (2001) 1–6;
(e) L. Brammer, E.A. Bruton, P. Sherwood, Cryst. Growth Des. 1 (2001) 277–290;
(f) Y.-R. Zhong, M.-L. Cao, H.-J. Mo, B.-H. Ye, Cryst. Growth Des. 8 (2008) 2282–2290.

[21] I. Hyla-Kryspin, G. Haufe, S. Grimme, Chem. Eur. J. 10 (2004) 3411–3422.

[22] (a) F.A. Cotton, L.M. Daniels, G.T. Jordan IV, C.A. Murillo, Chem. Commun. (1997) 1673–1674;
(b) A.N.M.M. Rahman, R. Bishop, D.C. Craig, M.L. Scudder, Eur. J. Org. Chem. (2003) 72–81.

[23] W.J. Geary, Coord. Chem. Rev. 7 (1971) 81–122.

[24] R. Mukherjee, Coord. Chem. Rev. 203 (2000) 151–218.

[25] T.K. Lal, R. Mukherjee, Polyhedron 16 (1997) 3577–3583.

[26] (a) R.J. Restivo, G. Ferguson, D.J. O'Sullivan, F.J. Lalor, Inorg. Chem. 14 (1975) 3046–3052;
(b) W. Luginbühl, P. Zbinden, P.A. Pittet, T. Armbruster, H.-B. Bürgi, A. E. Merbach, A. Ludi, Inorg. Chem. 30 (1991) 2350–2355;
(c) F.B. McCormick, D.D. Cox, W.B. Gleason, Organometallics 12 (1993) 610–612;
(d) H. Asano, K. Katayama, H. Kurosawa, Inorg. Chem. 35 (1996) 5760–5761;
(e) S. Bhambri, D.A. Tocher, J. Chem. Soc. Dalton Trans. (1997) 3367–3372;
H. Kurosawa, H. Asano, Y. Miyaki, Inorg. Chim. Acta 270 (1998) 87–94;
(g) H. Brunner, Th Zwack, M. Zabel, Z Kristallogr. NCS 217 (2002) 551–553;
(h) W. Lackner, C.M. Standfest-Hauser, K. Mereiter, R. Schmid, K. Kirchner, Inorg. Chim. Acta 357 (2004) 2721–2727.